

UNCLASSIFIED

AD NUMBER
AD130938
NEW LIMITATION CHANGE
TO Approved for public release, distribution unlimited
FROM Distribution authorized to U.S. Gov't. agencies and their contractors; Administrative/Operational Use; Mar 1956. Other requests shall be referred to Director, Wright Air Development Center, Wright-Patterson AFB, OH 45433.
AUTHORITY
AFSC ltr, 10 Aug 1967

THIS PAGE IS UNCLASSIFIED

WADC TECHNICAL REPORT 53-180

PART III

ASTIA DOCUMENT No. AD 130938

D-1791

RECEIVED  
MAY 1956  
FILE 070

INDEXED BY WCOSI

28,486

# STUDY OF MINIATURE ENGINE-GENERATOR SETS

## PART III DESIGN PROCEDURE OF SMALL HIGH-SPEED DC GENERATORS

KWAN Y. TANG  
OTTO LASTER

THE OHIO STATE UNIVERSITY RESEARCH FOUNDATION

MARCH 1956

This report is not to be announced or distributed  
automatically in accordance with AFR 205-43A,  
paragraph 6d.

2003 0623 004

WRIGHT AIR DEVELOPMENT CENTER

Statement A  
Approved for Public Release

## NOTICES

When Government drawings, specifications, or other data are used for any purpose other than in connection with a definitely related Government procurement operation, the United States Government thereby incurs no responsibility nor any obligation whatsoever; and the fact that the Government may have formulated, furnished, or in any way supplied the said drawings, specifications, or other data, is not to be regarded by implication or otherwise as in any manner licensing the holder or any other person or corporation, or conveying any rights or permission to manufacture, use, or sell any patented invention that may in any way be related thereto.

-----

Qualified requesters may obtain copies of this report from the ASTIA Document Service Center, Knott Building, Dayton 2, Ohio.

-----

This report has been released to the Office of Technical Services, U. S. Department of Commerce, Washington 25, D. C., for sale to the general public.

-----

Copies of WADC Technical Reports and Technical Notes should not be returned to the Wright Air Development Center unless return is required by security considerations, contractual obligations, or notice on a specific document.

WADC TECHNICAL REPORT 53-180  
PART III  
ASTIA DOCUMENT No. AD 130938

**STUDY OF MINIATURE ENGINE-GENERATOR SETS**  
PART III DESIGN PROCEDURE OF SMALL HIGH-SPEED DC GENERATORS

*KWAN Y. TANG*  
*OTTO LASTER*

*THE OHIO STATE UNIVERSITY RESEARCH FOUNDATION*

*MARCH 1956*

**EQUIPMENT LABORATORY**  
**CONTRACT No. AF 18(600)-192**  
**RDO No. 656-2112**

**WRIGHT AIR DEVELOPMENT CENTER**  
**AIR RESEARCH AND DEVELOPMENT COMMAND**  
**UNITED STATES AIR FORCE**  
**WRIGHT-PATTERSON AIR FORCE BASE, OHIO**

Carpenter Litho & Prtg. Co., Springfield, O.  
300 - November 1957

**Best Available Copy**

## FOREWORD

This report was prepared in the Mechanical Engineering Department of the Ohio State University under Contract No. AF 18(600)-192 "Study of Miniature Engine -- Generator Sets" with The Ohio State University Research Foundation. The project was initiated, administered, and directed by the Equipment Laboratory, with Dr. Erwin Naumann acting as project engineer.

The WADC Technical Report 53-180 Part II, submitted in December 1954, covered the basic engine investigation of the project. The aim of this report is to cover the investigation of a procedure which may be used for the design and development of 120-volt, 12,000 rpm, d-c flat-compounded generators of ratings from 35 to 400 watts. Procedure for the design and development of 400-cycle and 800-cycle generators will be studied during the remaining part of the present program.

The study will be completed with two additional reports:

Part IV - "Investigation of altitude and Low Temperature Performance; Starting, Cooling, Carburetion, Controls Systems; Noise Reduction", October 1956.

Part V - "Summary Report: Feasibility" October 1956.

## ABSTRACT

A procedure has been developed which will be helpful in the design of 120-volt, 12,000 rpm, d-c flat-compounded generators of ratings from 35 to 400 watts. This procedure includes the usual basic generator equations, empirical curves, and empirical relations. The empirical curves and empirical relations were obtained from commercial laminations and generators developed at The Ohio State University. The method outlines the steps in estimating the dimensions of the armature and field laminations, the stack length, the armature winding, the number of commutator bars and brushes, the shunt and series field coils and the predicted curve of terminal voltage versus load current.

## PUBLICATION REVIEW

The publication of this report does not constitute approval by the Air Force of the findings or the conclusions contained therein. It is published only for the exchange and stimulation of ideas.

FOR THE COMMANDER:



J. E. ROWLAND  
Chief, Systems & Power  
Conversion Section  
Electrical Branch  
Equipment Laboratory

# CONTENTS

	<u>Page</u>
GENERAL	1
I Introduction	1
II Design Manual	1
III Developed Generators	2
IV Brief Descriptions of Sections	2
V Merit of Design Manual	4
VI Symbols	5
1. PHYSICAL DIMENSIONS OF GENERATORS	6
1.1 Introduction	6
1.2 Generator Equations	6
1.3 Empirical Curves	7
1.4 Armature Diameter and Stack Length	9
1.5 Armature Lamination	11
1.6 Field Lamination	14
2. ARMATURE WINDING	17
2.1 Introduction	17
2.2 Type of Armature Winding	17
2.3 Number of Armature Conductors	17
2.4 Size of Armature Conductors	19
2.5 Armature Resistance	21
3. NO-LOAD SATURATION CURVE AND NO-LOAD $E_g$ VS $NI$ CURVE	22
3.1 Introduction	22
3.2 No-Load Saturation Curve	22

3.3	Air Gap Saturation Curve	23
3.4	Armature Teeth Saturation Curve	24
3.5	Armature Core Saturation Curve	25
3.6	Yoke Saturation Curve	26
3.7	Total No-Load Saturation Curve	26
3.8	No-Load $E_g$ vs NI Curve	26
4.	SHUNT FIELD WINDING	28
4.1	Introduction	28
4.2	Short Shunt versus Long Shunt	28
4.3	Wire Size of Shunt Field Coils	29
4.4	Number of Shunt Field Turns	31
4.5	Actual Shunt Field Resistance	32
5.	SERIES FIELD WINDING	33
5.1	Introduction	33
5.2	Series Field Wire Size	33
5.3	Armature Reaction Voltage Drop	34
5.4	Full-Load Generated Voltage	35
5.5	Number of Series Field Turns	36
6.	TERMINAL VOLTAGE VS LOAD CURRENT CURVE	39
6.1	Introduction	39
6.2	Terminal Voltage vs Load Current Curve	39
	NOMENCLATURE	41
	APPENDIX	45

## ILLUSTRATIONS

Figure No.	<u>Page</u>
A Disassembled View of 150-watt, 120-volt, 12,500 RPM DC Generator .....	3
B Dynamometer Test Bench .....	3
1-1 Armature Ampere-Conductors vs Ratio of Output Power Over Armature Speed .....	8
1-2 Ampere-Conductors per Inch of Armature Circumference vs Power Output .....	8
1-3 Output Coefficient vs Output Power .....	10
1-4 Air Gap Flux Density vs Armature Diameter .....	10
1-5 Armature Lamination .....	12
1-6 Tooth Tip Thickness vs Armature Diameter .....	13
1-7 Inside Armature Diameter vs Armature Diameter ....	14
1-8 Field Lamination .....	15
2-1 Developed Diagram of Typical Armature Winding, 13 Slots, 26 Commutator Bars, 4 Coil Sides per Slot	18
2-2 Current Density in Armature Conductors vs Output Power .....	20
3-1 Typical No-Load Saturation Curves .....	23
3-2 Tooth Cross-Section .....	25
4-1 Shunt Field Connections .....	28
4-2 Terminal Voltage vs Load Current Curves for a 400-watt, 12,250 RPM Generator .....	29
4-3 No-Load Generated Voltage vs Ampere-Turns per Pair of Poles .....	30
4-4 Current Density in Shunt Field Conductors vs Output Power .....	31
5-1 Current Density in Series Field Conductors vs Output Power .....	34

Figure No.		<u>Page</u>
5-2	No-Load Total and Teeth Plus Air-Gap Generated Voltages vs Ampere-Turns per Pair of Poles .....	35
5-3	No-Load Generated Voltage vs Ampere-Turns per Pair of Poles .....	37
6-1	Generated Voltage vs Ampere Turns per Pair of Poles	40

## NOMENCLATURE

a	Number of parallel armature paths
$A_c$	Cross sectional area of flux path in armature core (inches <sup>2</sup> )
$A_{ca}$	Approximate cross sectional area of an armature conductor (inches <sup>2</sup> )
$A_{cse}$	Cross sectional copper area of the series field coil (inches <sup>2</sup> )
$A_{sh}$	Cross sectional area of a shunt field coil (inches <sup>2</sup> )
$A_{TS}$	Area of specified armature tooth surface (inches <sup>2</sup> )
$A_{TW}$	Tooth width of specified armature tooth (inches)
$A_y$	Yoke cross sectional area (inches <sup>2</sup> )
$b_s$	Slot opening (inches)
$B_g$	Average air gap flux density (lines/inches <sup>2</sup> )
$B_{go}$	No-load air gap flux density (lines/inches <sup>2</sup> )
$B_{TS}$	Flux density of specified armature tooth surface (lines/inches <sup>2</sup> )
$B_{TW}$	Flux density in tooth width section of specified armature tooth surface (lines/inches <sup>2</sup> )
$B_y$	Yoke flux density (lines/inches <sup>2</sup> )
$B_{yo}$	No-load yoke flux density (lines/inches <sup>2</sup> )
C	Output coefficient in terms of rated power output (watts/rpm inches <sup>3</sup> )
$C^1$	Output coefficient in terms of internal developed power (watts/rpm inches <sup>3</sup> )
$C_1$	Carter's coefficient
$D_a$	Armature diameter (inches)
$D_{ai}$	Inside diameter of armature lamination (inches)
$D_{csh}$	Diameter of shunt field coil over the insulation (inches)
$D_o$	Outside diameter of yoke (inches)

NOMENCLATURE CON'T

$E_g$	Generated voltage (volts)
$E_{go}$	No-load generated voltage (volts)
$F_{sh}$	Fill factor of shunt field
$I_a$	Armature current (amperes)
$I_L$	Load current (amperes)
$I_{sh}$	Shunt field current (amperes)
$I_{sho}$	No load shunt field current (amperes)
$(I_a)_{FL}$	Full load armature current (amperes)
$(I_L)_{FL}$	Rated load current (amperes)
$J_a$	Armature conductor current density (amperes/inch <sup>2</sup> )
$J_{se}$	Series field coil current density (amperes/inch <sup>2</sup> )
$J_{sh}$	Shunt field coil current density (amperes/inch <sup>2</sup> )
$L_c$	Length of flux path in armature core (inches)
$L_g$	Length of air gap (inches)
$L_s$	Stack length of armature and field laminations (inches)
$L_T$	Tooth length (inches)
$L_y$	Length of flux path in yoke (inches)
$(LMT)_a$	Mean length turn of an armature coil (inches)
$(LMT)_{se}$	Mean length turn of the series field coil (inches)
$(LMT)_{sh}$	Mean length turn of the shunt field coil (inches)
$n$	Rated speed (rpm)
$N_{se}$	Number of series field turns
$N_{sh}$	Number of shunt field turns

NOMENCLATURE CON'T

NI	Ampere-turns per pair of poles
$(NI)_c$	Cross magnetizing ampere-turns per pair of poles
$(NI)_g$	Air gap ampere-turns per pair of poles
p	Number of poles
$P_T$	Tooth pitch (inches)
q	Ampere conductors per inch of armature circumference (amperes/inch)
r	Radius of field coil slot (inches)
$r_a$	Resistance per inch of an armature conductor (ohm/in)
$R_a$	Armature resistance (ohms)
$R_{at}$	Armature resistance at any temperature t (ohms)
$R_{a25}$	Armature resistance at 25°C (ohms)
$R_{(LMT)_{sh}}$	Resistance of a mean shunt-field turn (ohms)
$R_{se}$	Total series-field resistance (ohms)
$R_{sh}$	Total shunt-field resistance (ohms)
S	Number of slots
t	Temperature (Deg. C)
$T_T$	Tooth tip thickness (inches)
$(TPC)_a$	Turns per armature coil
$(TSC)_a$	Number of teeth spanned by one armature coil

NOMENCLATURE CON'T

$V_{AR}$	Armature reaction voltage drop (volts)
$V_B$	Brush contact voltage drop
$V_t$	Terminal voltage (volts)
$(V_t)_{FL}$	Rated terminal voltage (volts)
$V_{t0}$	No-load terminal voltage (volts)
$W_i$	Internal developed power (watts)
$W_o$	Rated power output (watts)
$W_T$	Tooth width (inches)
$Y$	Yoke thickness (inches)
$Z$	Total number of armature conductors
$\alpha$	Angle defined on Figure 1
$\Delta$	Thickness of pole tip (inches)
$\rho_{sht}$	Resistance per inch of the shunt field wire at any temperature $t$ (ohms/inch)
$\rho_{sh60}$	Resistance per inch of the shunt field wire at $60^\circ C$ (ohms/inch)
$\rho_{se}$	Resistance per inch of the series field wire (ohms/inch)
$\phi$	Flux (lines)
$\phi_o$	No-load flux (lines)
$\gamma$	Pole enclosure = pole arc/pole pitch

# DESIGN PROCEDURE OF SMALL HIGH-SPEED DC GENERATORS

## GENERAL

### I. INTRODUCTION

The purpose of this report is to cover the investigation of a procedure which may be useful in the design and development of 120-volt, d-c flat-compounded generators of ratings from 35 to 400 watts. The speed of these generators should be around 12,000 rpm (say, from 10,000 to 15,000 rpm).

A search of the literature indicated that very little has been written on these small high-speed d-c generators. A study of the small high-speed commercial series motors helped considerably in the development of a design procedure. From the study of the literature and commercial machines, it appears that generators of this voltage, power, and speed ratings usually have two poles (very low-voltage generators may have four poles). Also, the armature winding is usually lap wound; and thus the number of parallel paths will be two for a two-pole generator. A reason for using two poles is that only two brushes will be necessary, minimizing the brush friction loss of these high-speed generators. Another reason is that the two-pole construction is less expensive than the four-pole construction.

Thus, the design procedure will be limited to 120-volt, d-c flat-compounded, two-pole, lap-wound generators of ratings from 35 watts to 400 watts. The speed should be around 12,000 rpm. No interpoles will be used because of space limitation. The brushes are set midway between the two main poles primarily for rotation in either direction.

### II. DESIGN MANUAL

The design manual will give a procedure in estimating the dimensions of the armature and field laminations, the stack length, the armature winding, the number of commutator bars and brushes, the shunt and series field windings, and the predicted curve of terminal voltage versus load current.

The procedure consists of the following six major sections:

1. Physical Dimensions of Generators (including the dimensions of the armature and field laminations).
2. Armature Winding.

3. No-load Saturation Curve and No-load  $E_g$  vs. NI Curve.
4. Shunt Field Winding.
5. Series Field Winding.
6. Terminal Voltage vs. Load Current Curve.

Brief descriptions of these sections will be given in Article 4. The detailed descriptions will be given in the remainder of the report.

### III. DEVELOPED GENERATORS

It was necessary to obtain empirical curves and empirical relations, in addition to the usual generator equations, for estimating the physical dimensions of the generator, the armature winding, the field windings, etc. The usual generator equations are those normally found in design manuals of large machines and textbooks, such as, the equations for generated voltage and the power output. The empirical curves, such as those given in Figs. 1-1 through 1-4, and the empirical relations, such as equations (1-11) and (1-13), were obtained from commercial laminations and generators developed at The Ohio State University.

The three developed generators had power ratings of 150, 200, and 400 watts, and they were 120-volt, d-c flat-compounded, two-pole, lap-wound, approximately 12,000 rpm machines with efficiencies ranging from 50% to 57%. The developed generators were of the semienclosed type and contained internal fans. These generators were tested at ground level conditions and were considered satisfactory when they had acceptable terminal voltage variation from no-load to full-load, (say, the no-load voltage is about 3 volts higher than the full-load voltage and the intermediate-load voltage is about 5 volts higher than the full-load voltage, as indicated in Fig. 4-2) temperature rise of about 55° C. above an approximate ambient temperature of 25° C, and sufficiently good commutation as determined by visual observation. Figure A is a disassembled view of a typical developed generator. Figure B shows the setup with dynamometers for testing the developed generators at ground level conditions.

### IV. BRIEF DESCRIPTIONS OF SECTIONS

Section 1, Physical Dimensions of Generators, gives generator equations, empirical curves, empirical relations and procedure for determining the dimensions of the armature lamination as shown in Fig. 1-5, the dimensions of the field lamination as given in Fig. 1-8, and the stack length as indicated in equation (1-10).

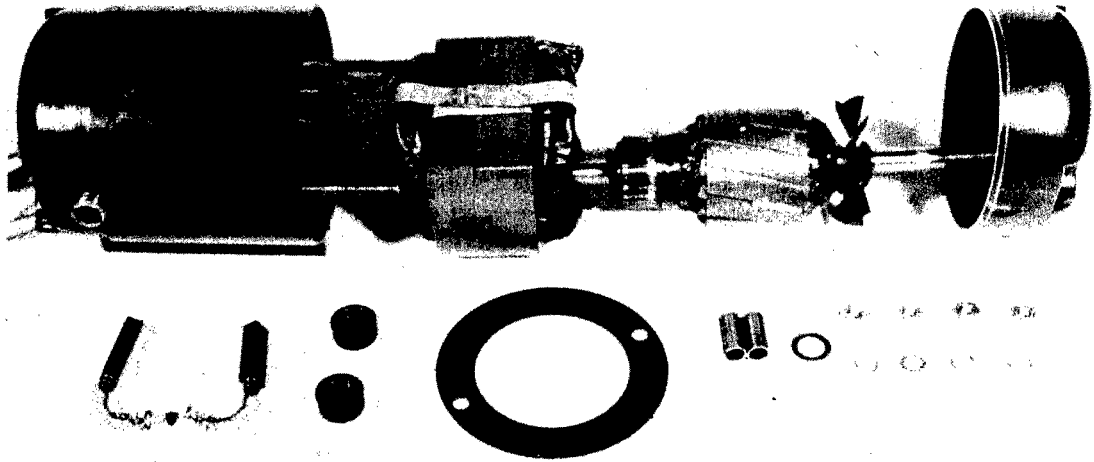


FIG. A. DISASSEMBLED VIEW OF 150-WATT, 120-VOLT, 12500 RPM DC GENERATOR.

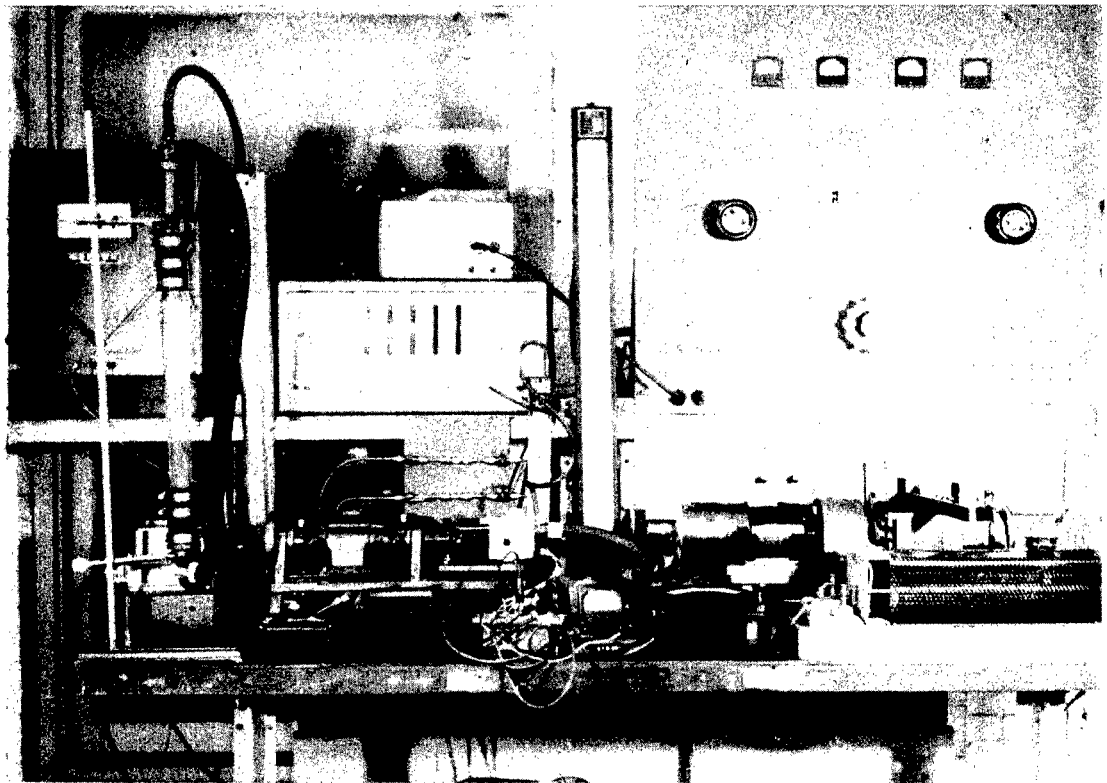


FIG. B. DYNAMOMETER TEST BENCH.

Section 2, Armature Winding, suggests a type of armature winding which is simplex, progressive, lap-wound, and with four coil sides per slot. With four coil sides per slot, the number of commutator bars is twice the number of armature slots. The end connections are so arranged that the brushes can be set midway between the main poles. This section outlines methods of determining the number of armature conductors, the size of the armature conductors, and the total resistance of the armature.

Section 3, No-load Saturation Curve and No-load  $E_g$  vs. NI Curve, indicates the procedures for determining saturation curves of the different parts of the magnetic circuit and then the method for combining these curves to obtain the total no-load saturation curve. For any specified speed, the no-load  $E_g$  vs. NI curve can be found quite readily with the aid of the no-load saturation curve as shown in Fig. 3-1 and the generated voltage equation (1-2).

Section 4, Shunt Field Winding, recommends that the compound generators be connected short shunt as shown in Fig. 4-1(a). The procedures for determining the size of wire for the shunt field, the number of turns for the shunt field coils, and the actual shunt field resistance are also given.

Section 5, Series Field Winding, presents methods for estimating the wire size of the series field winding, the armature reaction, and the number of series field turns.

Section 6, Terminal Voltage vs. Load Current Curve, describes a procedure for calculating the different points on the terminal voltage vs. load current curve. Such a curve will show the variation of the terminal voltage from no load to full load.

## V. MERIT OF DESIGN MANUAL

It should be emphasized that no actual generator has been designed and built from the procedure given in this design manual. The merit of the manual will depend on how the calculated data check the test data of generators designed from the suggested procedure. If the calculated values and the test values do not check satisfactorily, then some modifications on the empirical curves and empirical equations will be necessary to improve the design procedure.

It should also be mentioned that the design manual does not include any considerations of the behavior of the generators at different altitudes (this will depend on the altitudes at which the engines may be operated), the configurations for best heat transfer, the problem of cooling, the calculation method of iron losses, the use of permanent magnets, and a good analytical method for determining satisfactory commutation.

## VI. SYMBOLS

All symbols and their definitions are given at the end of the design manual for convenience.

# 1. PHYSICAL DIMENSIONS OF GENERATORS

## (Armature and Field Laminations)

### 1.1 Introduction

Before the design of small high-speed generators can be started for the usual ground-level conditions, the following specifications must be given:

- (a) Rated power output ( $W_o$ )
- (b) Rated terminal voltage ( $V_t$ )<sub>FL</sub>
- (c) Rated speed in rpm ( $n$ )

Then reasonable estimates of the stack length and the dimensions of the armature and field laminations may be obtained with the aid of the usual generator equations, empirical relations, and empirical curves.

### 1.2 Generator Equations

Useful generator equations will now be considered. The fundamental equation for the generated voltage of d-c generators is

$$E_g = \frac{Z \phi n p 10^{-8}}{60 a} \quad (1-1)$$

For two-pole generators,  $p=2$  and  $a=2$ , equation (1-1) becomes

$$E_g = \frac{Z \phi n 10^{-8}}{60} \quad (1-2)$$

The average air-gap flux density  $B_g$  may be obtained from the total pole flux  $\phi$  and the approximate area of the pole face. Thus,

$$B_g = \frac{\phi}{\pi D_a L_s \gamma} = \frac{2\phi}{\pi D_a L_s \gamma} \quad (1-3)$$

where  $L_s$  is the stack length assumed to be the same for both field and armature and the pole enclosure  $\gamma$  of two-pole generators is between 0.55 and 0.68 of pole pitch.

The ampere-conductors per inch of armature circumference is designated by the symbol  $q$ . If  $I_a/2$  is the full-load current through each armature conductor, then  $q$  is equal to the ratio of full-load armature ampere-conductors  $ZI_a/2$  to the circumference of the armature  $\pi D_a$ , or

$$q = \frac{Z I_a}{2 \pi D_a} \quad (1-4)$$

The internal developed power of the generator is

$$W_i = E_g I_a = \frac{Z \phi n I_a 10^{-8}}{60} \quad (1-5)$$

With the aid of equations (1-3 and (1-4), equation (1-5) may be written

$$W_i = D_a^2 L_s n \left( \frac{B_g q \gamma \pi^2}{60 \times 10^8} \right) = D_a^2 L_s n (C') \quad (1-6)$$

where  $C'$  is known as an output coefficient. For practical applications, it is more convenient to use an empirical coefficient  $C$  in terms of the rated output power  $W_o$ , namely

$$C = \frac{W_o}{D_a^2 L_s n} \quad (1-7)$$

where  $W_o$ ,  $D_a$ ,  $L_s$  and  $n$  are obtained from the developed generators.

### 1.3 Empirical Curves

Important parts of the design procedure are the empirical curves and the empirical relations derived from the developed generators. Figures 1-1 through 1-4 show empirical curves which are used for estimating the stack length and the dimensions of the armature and field laminations. The data used for plotting the full-line portions of these curves were obtained from the generators developed at The Ohio State University. The points marked  $x$  on these curves were based on a calculated 50-watt, 120-volt, 2-pole, lap-wound, d-c flat-compounded, 13,000 rpm generator.

Figure 1-1 shows an empirical curve of armature ampere-conductors ( $Z I_a/2$ ) versus the ratio of rated output power to speed ( $W_o/n$ ). The quantities  $Z$ ,  $I_a$ ,  $W_o$  and  $n$  are known for each of the developed generators.

Figure 1-2 is an empirical curve of armature ampere-conductors per inch of armature circumference ( $q = Z I_a/2 \pi L_a$ ) versus the rated output power  $W_o$ . The quantities  $Z$ ,  $I_a$ ,  $D_a$  and  $W_o$  are obtained from each of the developed generators.

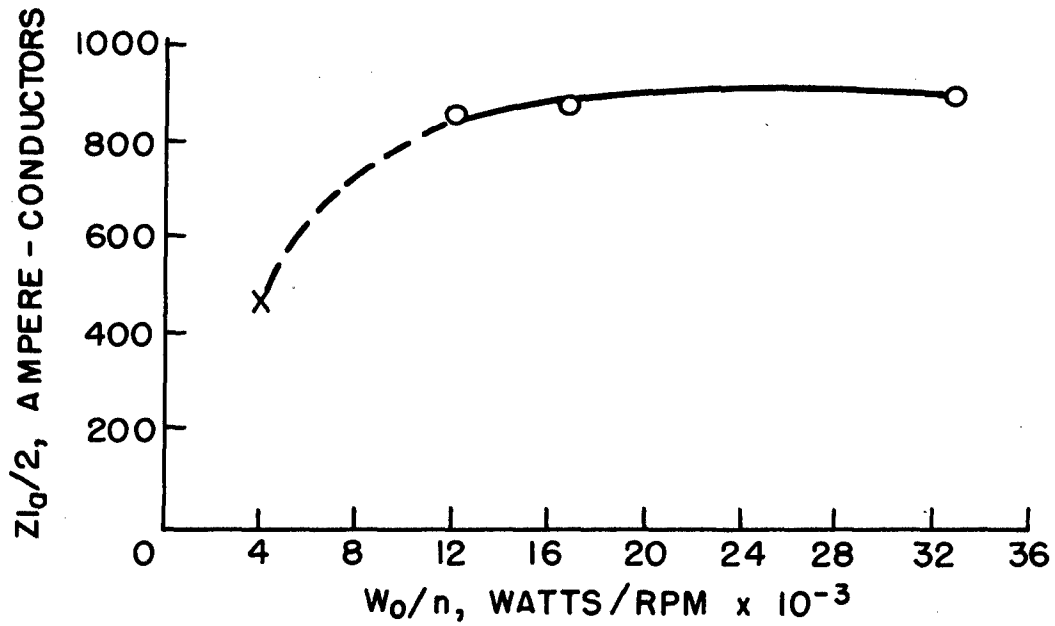


FIG. 1-1. ARMATURE AMPERE - CONDUCTORS VS. RATIO OF OUTPUT POWER OVER ARMATURE SPEED

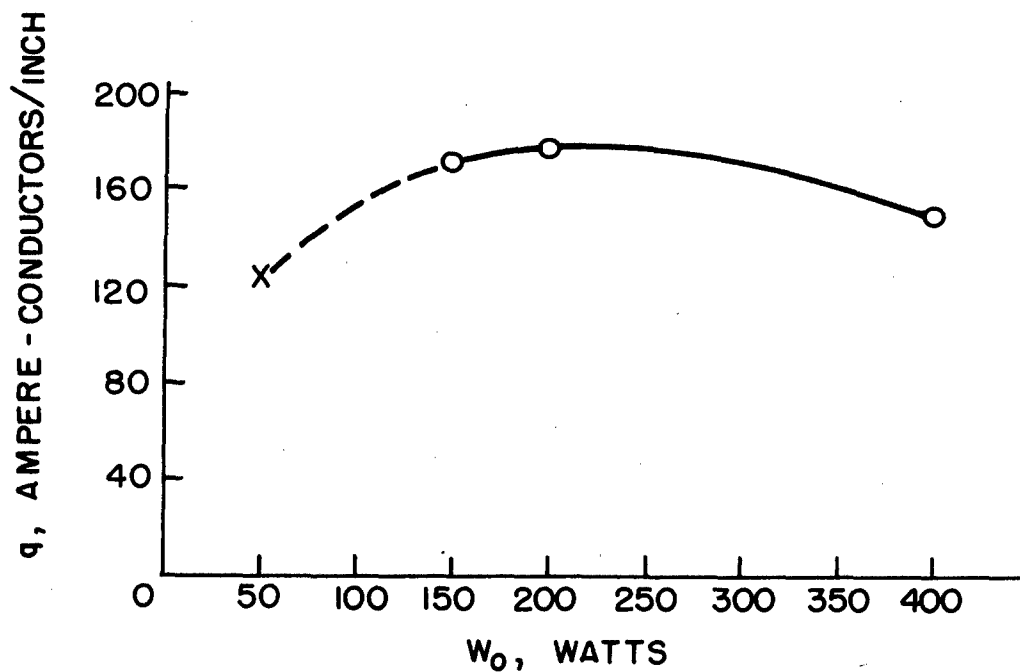


FIG. 1-2. AMPERE - CONDUCTORS PER INCH OF ARMATURE CIRCUMFERENCE VS. POWER OUTPUT

An empirical curve of output coefficient (C) versus rated output power ( $W_o$ ) is given in Figure 1-3. This curve is derived from equation (1-7). For each developed generator,  $W_o$ ,  $D_a$ ,  $L_s$ , and  $n$  are known.

Figure 1-4 is an empirical curve of no-load air gap flux density ( $B_{go}$ ) versus armature diameter ( $D_a$ ). It is obtained from an empirical relation which will now be derived. The no-load generated voltage  $E_{go}$  is slightly higher than the no-load terminal voltage  $V_{to}$ . For each developed generator,  $V_{to}$  can be measured by operating the machine at rated no-load conditions. As a good engineering approximation, it is assumed that  $E_{go} = V_{to}$ . Then from equations (1-2) and (1-3)

$$B_{go} = \frac{120 V_{to} 10^8}{\pi Z D_a L_s \gamma n} \quad (1-8)$$

#### 1.4 Armature Diameter and Stack Length

The armature diameter and stack length may be found in the following manner.

##### (a) Armature Diameter

- (1) For  $\frac{W_o}{n}$ , find  $\frac{Z I_a}{2}$  from Figure 1-1
- (2) For  $W_o$ , find  $q = \frac{Z I_a}{2\pi D_a}$  from Figure 1-2
- (3) Knowing  $\frac{Z I_a}{2}$  and  $q$ , equation (1-4) gives the armature diameter, or

$$D_a = \frac{Z I_a}{2\pi q} \quad (1-9)$$

##### (b) Stack Length

- (1) For  $W_o$ , find  $C$  from Figure 1-3
- (2) Knowing  $W_o$ ,  $C$ ,  $D_a$  and  $n$ , equation (1-7) gives stack length, or

$$L_s = \frac{W_o}{C I_a^2 n} \quad (1-10)$$

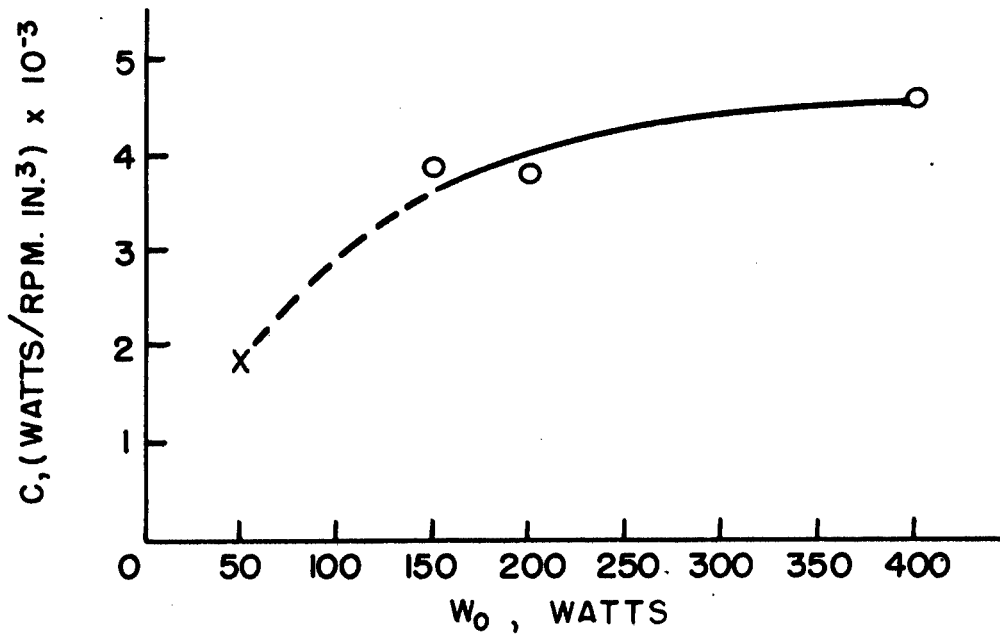


FIG. 1-3. OUTPUT COEFFICIENT VS. OUTPUT POWER

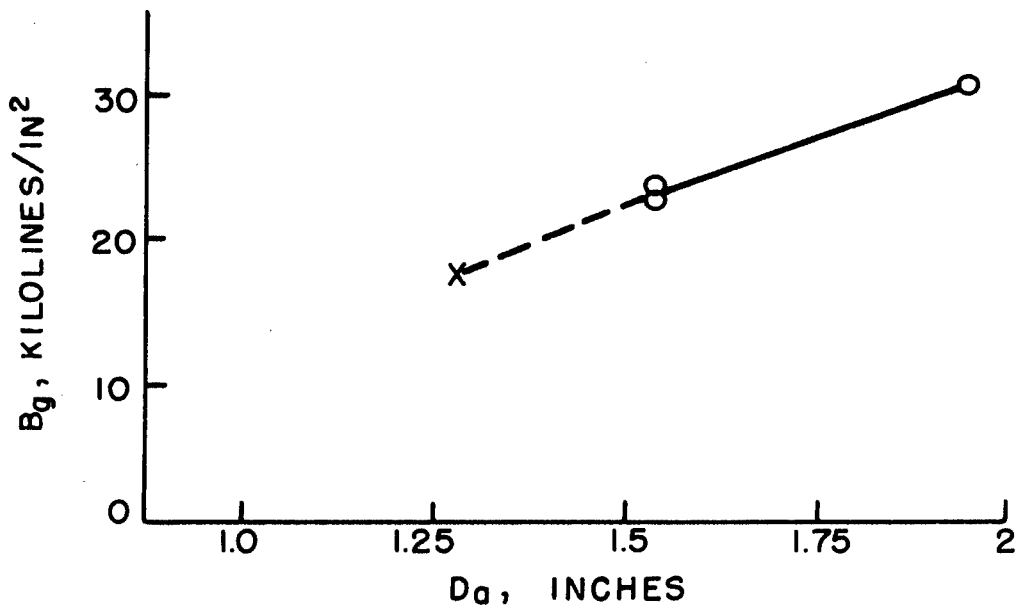


FIG. 1-4. AIR GAP FLUX DENSITY VS. ARMATURE DIAMETER

## 1.5 Armature Lamination

The dimensions of the armature lamination may be estimated in the following manner.

(a) Armature Diameter. - - The armature diameter

$$D_a = \frac{Z I_a}{2 \pi q} \quad (1-9)$$

is obtained from the method given in Article 1.4.

(b) Number of Armature Teeth. - - The number of teeth ( = number of slots S) may be found by first determining the tooth pitch  $P_T$ . From study of a large number of small commercial armature laminations, points of tooth pitch  $P_T$  versus armature diameter  $D_a$  were plotted. An approximate straight line through these points has the form

$$P_T = 0.2 + 0.117 D_a \quad (1-11)$$

The number of teeth ( = slots S) can be estimated from the expression

$$S = \frac{\pi D_a}{P_T} \quad (1-12)$$

If S found from equation (1-12) is not an integer, then the nearest whole number should be used for S. The corrected value of tooth pitch can be calculated by using the whole number of S in equation (1-12), or

$$P_T = \frac{\pi D_a}{S} \quad (1-12a)$$

(c) Teeth Configuration. - - Figure 1-5 shows a sketch of an armature lamination. By examination of a number of small commercial armature laminations, empirical relations and diagrams have been developed to estimate the tooth width  $W_T$ , the tooth length  $L_T$ , the tooth tip thickness  $t_T$ , the slot opening  $b_s$ , and the inside diameter of the armature lamination  $D_{ai}$ .

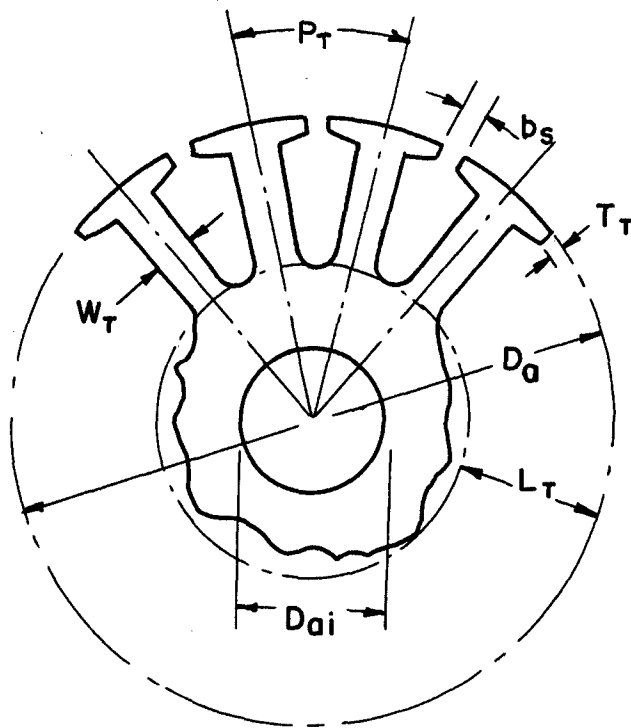


FIG. 1-5. ARMATURE LAMINATION

- (1) Tooth Width  $W_T$ . - It is assumed that the armature teeth have parallel sides as indicated in Figure 1-5. The examination of commercial armature laminations indicated that the tooth flux density is approximately from 3 to 5 times as high as the air gap flux density. Then

$$\begin{aligned}
 W_T &= (0.2 \text{ to } 0.33) \frac{\text{pole face area}}{\text{number of teeth under a pole}} \\
 &= (0.2 \text{ to } 0.33) \left\{ \frac{\pi D_a \gamma L_s}{2} \right\} \left\{ \frac{\pi D_a^2}{S \pi D_a \gamma L_s} \right\} \\
 &= (0.2 \text{ to } 0.33) \frac{\pi D_a}{S} \qquad (1-13)
 \end{aligned}$$

- (2) Tooth Length  $L_T$ . - The tooth length  $L_T$  is assumed to be that indicated in Figure 1-5. From examination of commercial laminations, a simple empirical relation for the tooth length is

$$L_T = \frac{W_T}{(0.2 \text{ to } 0.3)} \quad (1-14)$$

Attention is called to the fact that the factor (0.2 to 0.3) in equation (1-14) is not the same as the factor (0.2 to 0.33) in equation (1-13). Thus, a value selected in (0.2 to 0.3) need not be the same as the value selected in (0.2 to 0.33).

- (3) Tooth Tip Thickness  $T_T$ . - - Figure 1-5 shows a very simple tooth configuration with tooth tip thickness  $T_T$ . For a particular choice of tooth configuration, mechanical strength and other factors must be considered. From study of commercial laminations, points of  $T_T$  versus  $D_a$  are plotted in Figure 1-6. Some judgment must be used to select a  $T_T$  for a particular armature diameter  $D_a$ .

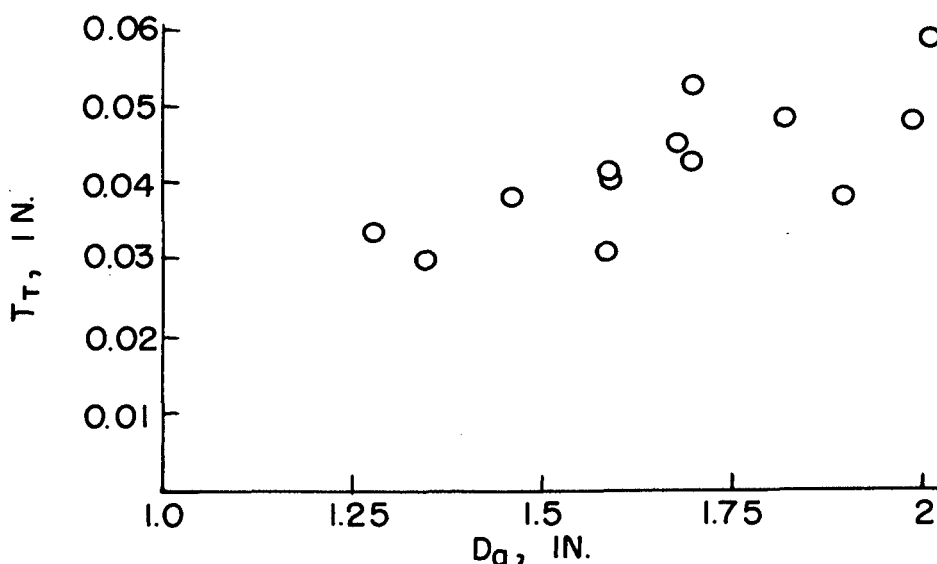


FIG. 1-6. TOOTH TIP THICKNESS VS. ARMATURE DIAMETER

- (4) Slot Opening  $b_s$ . - - Partially closed slots are recommended for 120-volt generators. The study indicated that the slot opening  $b_s$  is approximately equal to 21% of the tooth pitch  $P_T$ .
- (5) Inside Diameter  $D_{ai}$ . - - Figure 1-7 shows points of inside diameter  $D_{ai}$  of commercial armature lamination versus armature diameter  $D_a$ . The designer must exercise good judgment in selecting a minimum  $D_{ai}$  for any particular armature lamination.

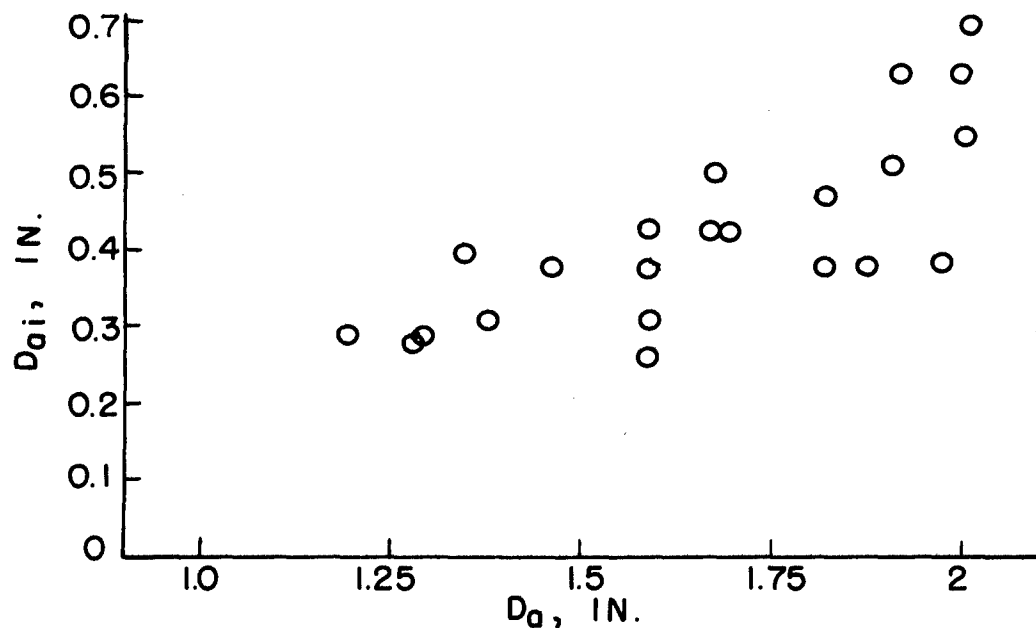


FIG. 1-7. INSIDE ARMATURE DIAMETER VS. ARMATURE DIAMETER

Whenever possible, it is recommended that the armature be skewed one slot pitch to minimize voltage ripple.

#### 1.6 Field Lamination

Figure 1-8 shows a round field lamination. If it is desirable to use a flat lamination, the outline of such a lamination may be imagined with the aid of the two horizontal dotted lines. It can be shown by calculations that the generator characteristics obtained from these two types of laminations are nearly the same. For clearness, the design procedure will be limited to the round lamination.

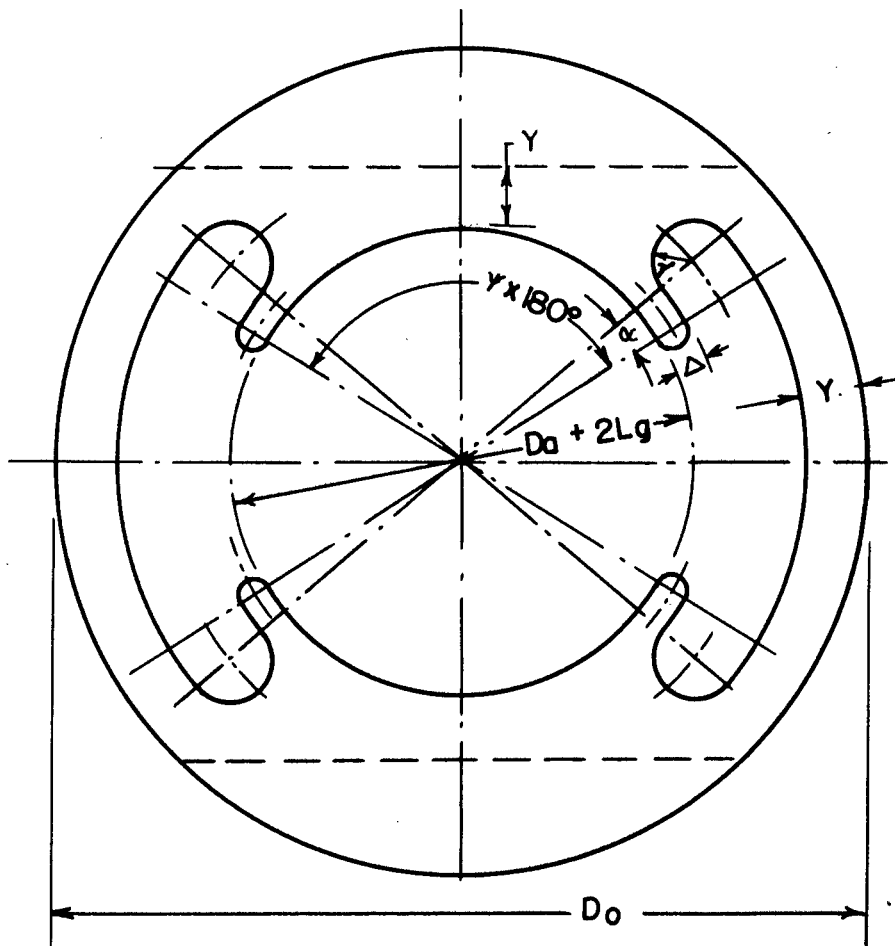


FIG. 1-8. FIELD LAMINATION

The design of a field lamination involves the air gap length, the dimensions of the pole, the section for the shunt and series field coils, and the thickness of the yoke. Empirical dimensions and flux densities for some parts of the lamination were obtained with the aid of commercial laminations and the generators developed at The Ohio State University. These are given below.

The air gap length,  $L_g$  varies from 0.012 to 0.015 inch. Then the inside diameter of the field lamination (at the pole arcs) is  $(D_a + 2 L_g)$ .

The pole enclosure  $\gamma$  of two-pole generators is between 0.55 to 0.68 of pole pitch.

The shape of the field pole may be estimated in the following way. The minimum thickness of the pole tip  $\Delta$  shown in Figure 1-8 should be about 1/16 inch. The tip may be rounded with a radius of about 1/32 inch. The section for the shunt and series field coils is defined as the space between the pole tip and the inside surface of the yoke. An expression for the radius  $r$  of this section in Figure 1-8 may be derived in the following manner.

$$\left(\frac{D_a}{2} + L_g + \Delta + r\right) \sin \alpha = r$$

$$r = \frac{\left(\frac{D_a}{2} + L_g + \Delta\right) \sin \alpha}{1 - \sin \alpha} \quad (1-15)$$

where  $\alpha$  is defined in Figure 1-8 and it ranges between  $4^\circ$  and  $8^\circ$ .

The yoke thickness  $Y$  is dependent upon the flux through the yoke and the allowable flux density in the yoke  $B_y$ . From data on the developed generators, the no-load flux density in the yoke  $B_{yo}$  lies in the range from 75,000 to 85,000 lines per square inch. The no-load flux through the yoke,  $\phi_o/2$ , is equal to the product of the no-load air gap flux density  $B_{go}$ , Figure 1-4, and one-half of the pole face area. Also,  $\phi_o/2$  is equal to the product of  $B_{yo}$  and the yoke cross-sectional area  $A_y$ , or  $\phi_o/2 = B_{yo}A_y$ . Thus,

$$Y = \frac{A_y}{L_s} = \frac{\frac{\phi_o}{2 B_{yo}}}{L_s} = \frac{\frac{B_{go} \pi D_a L_s \gamma}{4 B_{yo}}}{L_s} = \frac{B_{go} \pi D_a \gamma}{4 B_{yo}} \quad (1-16)$$

When bolt holes are used, the thickness of the yoke at the bolt hole sections must be increased accordingly.

The outside diameter of the field lamination is

$$D_o = D_a + 2 L_g + 2 \Delta + 4 r + 2 Y \quad (1-17)$$

For the flat field lamination, the thickness of the pole at the center of the pole face is approximately equal to the yoke thickness as shown in Figure 1-8. This dimension depends on the size and location of the rivet holes when such holes are used around the pole sections for holding the laminations together.

## 2. ARMATURE WINDING

### 2.1 Introduction

The type of armature winding, number of commutator bars, coil pitch, number of armature conductors, the size of armature conductors, and the armature resistance will be considered in this section.

### 2.2 Type of Armature Winding

Satisfactory results were obtained from the 120-volt generators developed at The Ohio State University. The armature winding of each of these developed generators was simplex, progressive, lap wound and having four coil sides per slot. Four coil sides per slot were used because of the advantage in available slot space for the armature conductors and the mechanical strength of the armature lamination. Thus, based on the satisfactory results of the developed generators, the suggested type of armature winding is simplex, progressive, lap wound, and with four coil sides per slot.

With four coil sides per slot, the number of commutator bars is twice the number of slots  $S$ , or

$$\text{Number of commutator bars} = 2 S \quad (2-1)$$

where  $S$  obtained from equation (1-12) is corrected to a whole number.

In general, short-pitch coils are suggested. The number of teeth spanned by a full-pitch armature coil is  $S/2$ . For fractional-pitch winding, the coils are short pitched to the nearest slot under 180 electrical degrees. For example, if  $S = 13$  then a full-pitch coil will span  $13/2 = 6.5$  teeth and a short-pitch coil will span 6 teeth. The short pitching of the coils will, in general, improve commutation and simplify the actual winding of the armature.

Figure 2-1 shows a developed diagram of a lap winding with four coil sides per slot, 13 slots, and 26 commutator bars.

### 2.3 Number of Armature Conductors

The approximate number of armature conductors  $Z$  may be obtained from equation (1-2) or equation (1-8) and the no-load air gap flux density  $B_{go}$  from Figure 1-4. It has been assumed that  $E_{go} \approx V_{to}$ . Since the generators are to be flat-compounded, then  $V_{to} = (V_t)_{FL}$  and  $E_{go} \approx (V_t)_{FL}$ . Thus,

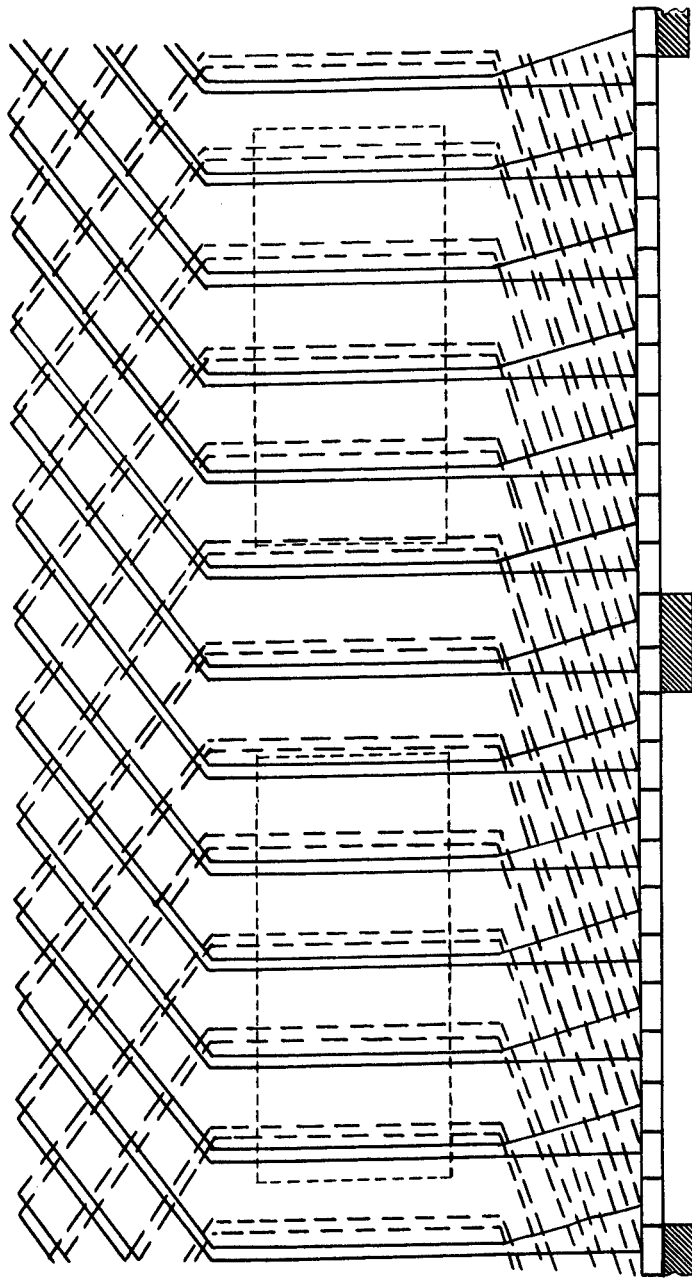


FIG. 2-1. DEVELOPED DIAGRAM OF TYPICAL ARMATURE WINDING,  
13 SLOTS, 26 COMMUTATOR BARS, 4 COIL SIDES PER SLOT

$$Z = \frac{120 (V_t)_{FL} 10^8}{B_{go} D_a L_s n} \quad (2-2)$$

With four coil sides per slot, the approximate number of turns per armature coil  $(TPC)_a$  is given by the expression

$$(TPC)_a = \frac{Z}{4S} \quad (2-3)$$

If  $(TPC)_a$  calculated from equation (2-3) is not an integer, then the nearest whole number should be used as the number of turns per armature coil. The exact number of armature conductors is

$$Z = 4S (TPC)_a \quad (2-4)$$

#### 2.4 Size of Armature Conductors

The net slot area is defined as the net winding space in a slot after deducting from the gross slot area the area required for the insulating cell and wedge. The net slot area can be calculated, but it is more easily determined by making a large scale layout of the slot with the insulating cell and wedge in place and measuring the net slot area.

The fill factor is defined as the ratio of the cross-sectional area of the wires including wire insulation in a slot to the net slot area. From the manufacturing standpoint on ease of winding, the fill factor for round wires should be approximately from 0.45 to 0.55.

The approximate cross-sectional area of an armature conductor (copper plus insulation) is

$$A_{ca} = \frac{(\text{net slot area}) (\text{fill factor})}{\text{number of armature conductors per slot}} \quad (2-5)$$

The selected standard commercial wire size should have a cross-sectional area closest to  $A_{ca}$ .

Figure 2-2 is a plot of allowable current densities in the armature conductors for 55° C rise above an approximate ambient temperature of 25° C. This curve may be used as a guide to determine whether the current density is "excessive" for the selected wire size. An "excessive" current density will mean a temperature rise greater than 55° C. The tolerable temperature rise will depend upon the life of the generator, the insulation used, the cooling, the altitude, etc. Thus, in the end, the designer must decide on the temperature rise.

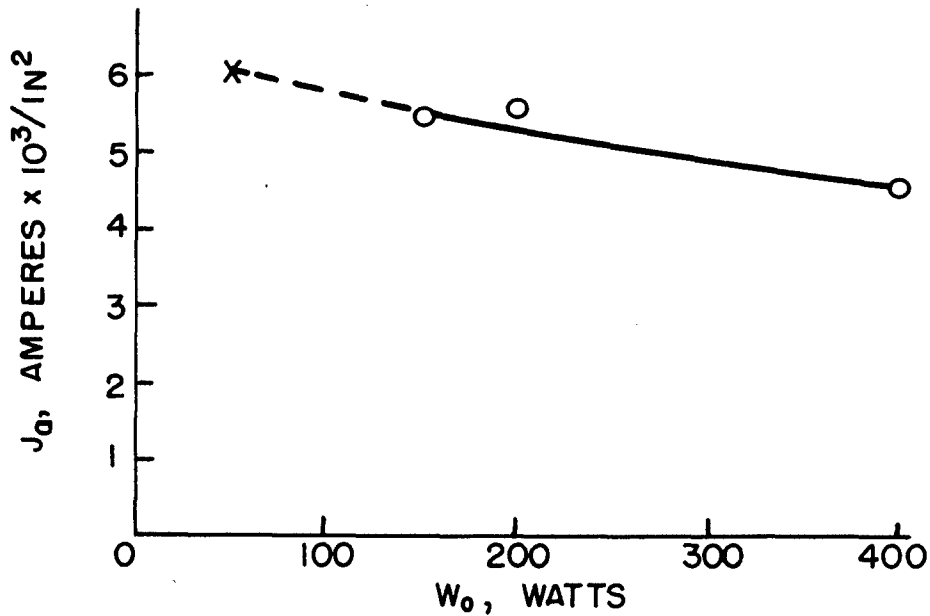


FIG. 2-2. CURRENT DENSITY IN ARMATURE CONDUCTORS VS. OUTPUT POWER

To determine the current density of the selected wire size, the full-load armature current  $(I_a)_{FL}$  must be found. The full-load armature current is equal to the sum of the rated load current  $(I_L)_{FL} = W_o / (V_t)_{FL}$  and the shunt field current  $I_{sh}$  at full load. Since the armature current density curve in Figure 2-2 will be used only as a guide, an approximate value for  $I_a$  will be sufficient at this point. From study of the developed generators, an approximation is to assume  $I_{sh} = 0.1 (I_L)_{FL}$ . Then

$$(I_a)_{FL} = 1.1 (I_L)_{FL} = 1.1 \frac{W_o}{(V_t)_{FL}} \quad (2-6)$$

and the current density in the armature conductors is equal to  $I_a/2$  divided by the cross-sectional copper area of the armature conductor.

If this calculated value of current density exceeds the value obtained from Figure 2-2 for a given power output, then the next larger size of wire should be used provided the fill factor is satisfactory from the standpoint of manufacturing. However, if the fill factor is too high, then a solution is to use the original wire size and to have more air through the completed generator. The amount of air required may be determined by a cut-and-try process or by calculation.

## 2.5 Armature Resistance

The resistance per armature path is equal to the length of wire per path in inches times the resistance per inch obtained from wire tables. The armature resistance is 1/2 of this value since there are two parallel paths in a two-pole generator. This will now be considered.

The length of a mean turn of an armature coil is designated by  $(LMT)_a$ . The  $(LMT)_a$  in inches may be obtained approximately from the following expression

$$(LMT)_a = 2 \left( L_s + \frac{(TSC)_a \pi (D_a - L_T)}{S} \right) \quad (2-7)$$

where  $(TSC)_a$  = number of teeth spanned by one armature coil.

The total length of wire per path in inches is equal to the product of  $(LMT)_a$  and the number of turns  $(Z/2 \times 1/2)$  per path. Thus,

$$\text{Length per path} = (LMT)_a \times \left( \frac{Z}{2} \times \frac{1}{2} \right) \quad (2-8)$$

The resistance per path is

$$\text{Resistance per path} = (LMT)_a \times \left( \frac{Z}{2} \times \frac{1}{2} \right) r_a \quad (2-9)$$

where  $r_a$  is the resistance per inch obtained from wire tables. If the wire table is for 25° C, then the resistance per inch is  $r_{a25}$ . With two parallel paths and at 25° C, the armature resistance  $R_a$  is

$$R_{a25} = \frac{(LMT)_a Z r_{a25}}{8} \quad (2-10)$$

and at any temperature  $t^\circ\text{C}$  is

$$R_{at} = R_{a25} \left( \frac{234.5 + t}{234.5 + 25} \right) \quad (2-11)$$

### 3. NO-LOAD SATURATION CURVE AND NO-LOAD $E_g$ VS NI CURVE

#### 3.1 Introduction

The no-load saturation curve and the no-load  $E_g$  vs NI curve are necessary for the determination of the shunt and series field coils and for the calculation of the terminal voltage versus load curve.

The no-load saturation curve is a relation between flux and ampere-turns per pair of poles. It can be calculated from the physical dimensions of the armature and field structures with the aid of the magnetization curve for the lamination iron.

The no-load  $E_g$  vs NI curve for any specified speed is a relation between the generated voltage  $E_g$  and the ampere-turns per pair of poles. It can be determined by using the no-load saturation curve and the generated voltage equation (1-2); that is, by using different values of  $\phi$  from the no-load saturation curve and calculating the corresponding generated voltages.

#### 3.2 No-load Saturation Curve

As considered in this design manual, the magnetic path of the generator consists of four major parts: air gap, teeth, armature core, and field yoke (which is assumed to account for the field poles). The consideration of the field poles as a separate major part would require flux mapping, which perhaps should be done for better accuracy. Since the pole flux density is relatively low and the pole length is short in the type of field lamination used here, a rough approximation is to include the pole ampere-turns in those of the yoke by increasing the length of the yoke path.

Figure 3-1 shows typical individual saturation curves and the typical total no-load saturation curve. Each of the individual saturation curves is obtained by assuming different values of  $\phi$  and calculating the corresponding ampere-turns required for that part of the magnetic circuit. The total no-load saturation curve is derived by adding the different ampere-turns for each value of  $\phi$ . The methods for calculating the ampere-turns of each part of the magnetic circuit will be presented in the following articles.

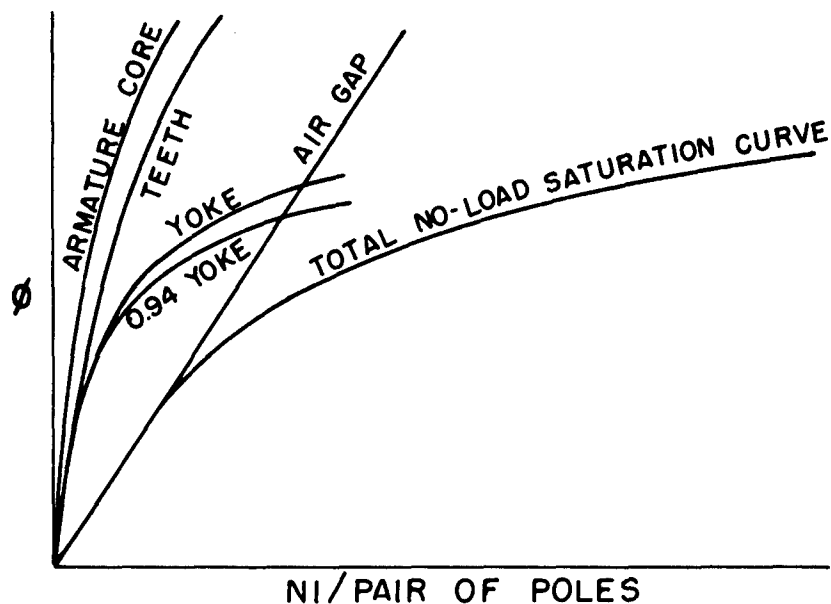


FIG. 3-1. TYPICAL NO-LOAD SATURATION CURVES

### 3.3 Air Gap Saturation Curve

The air gap saturation curve is a straight line passing through the origin. Hence, it is necessary only to assume a value of  $\phi$  and calculate the corresponding air gap ampere-turns  $(NI)_g$  per pair of poles.

Because of the presence of armature slots, the air gap length should be corrected. For partially closed slots, a simplification of Carter's coefficient equation gives a correction factor

$$C_1 = \frac{(4.4 L_g + 0.75 b_s) P_T}{(4.4 L_g + 0.75 b_s) P_T - b_s^2} \quad (3-1)$$

Then the corrected air gap length is

$$\text{Corrected air gap length} = C_1 L_g \quad (3-2)$$

The average air gap flux density  $B_g$  is equal to the flux  $\phi$  per pole divided by the pole face area, or

$$B_g = \frac{2\phi}{\pi D_a \gamma L_s} \quad (3-3)$$

The air gap ampere-turns per pair of poles to produce  $B_g$  is

$$(NI)_g = 2 \{ 0.313 B_g C_1 L_g \} \quad (3-4)$$

Thus, a point on the air gap saturation curve is determined by assuming  $\phi$ , then finding  $B_g$  from equation (3-3), and finally obtaining  $(NI)_g$  from equation (3-4). The air gap saturation curve is a straight line drawn through this point and the origin.

### 3.4 Armature Teeth Saturation Curve

Figure 3-2 shows a simple cross-section of an armature tooth with sections a and b. For more complicated configurations, more sections will be necessary. It is hoped that the simple configuration will illustrate the procedure in determining the armature teeth saturation curve.

A point on the armature teeth saturation curve may be determined in the following manner. First, assume a flux  $\phi$ . With the known values of the dimensions of the tooth, the stack length  $L_s$ , the pole enclosure  $\gamma$ , and the number of slots  $S$ , calculate the cross-sectional area of each section under a pole face. Thus,

$$\text{Tooth Surface } A_{TS} = \left(\gamma \frac{S}{2}\right) (P_T - b_g) (0.95 L_s) \quad (3-5)$$

$$\text{Tooth Width } A_{TW} = \left(\gamma \frac{S}{2}\right) W_T \times 0.95 L_s \quad (3-6)$$

where 0.95 is the stacking factor. The flux density for each section is

$$\text{Tooth Surface } B_{TS} = \frac{\phi}{A_{TS}} \quad (3-7)$$

$$\text{Tooth Width } B_{TW} = \frac{\phi}{A_{TW}}$$

From the magnetization curve of the lamination material, obtain the ampere-turns per inch for  $B_{TS}$  and  $B_{TW}$ . The total ampere-turns per pair of poles for each section is found by multiplying the proper ampere-turns per inch by the corresponding length  $2 L_a$  or  $2 L_b$ . The total ampere-turns for the entire tooth is the sum of the ampere-turns for section a and b.

Other points on the armature teeth saturation curve are similarly found by assuming different values for  $\phi$ .

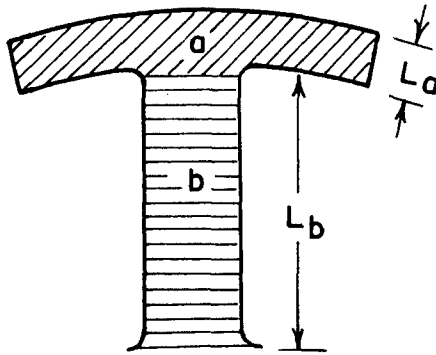


FIG. 3-2. TOOTH CROSS - SECTION

### 3.5 Armature Core Saturation Curve

Refer to Figure 1-5. The armature core is usually considered to be the volume of lamination iron between the circle with diameter  $(D_a - 2 L_T)$  and the inside diameter  $D_{ai}$ . If the flux penetration into the shaft is assumed to be 0.025 inch, then the total cross-sectional area of the armature core is

$$A_c = 0.95 \left\{ (D_a - 2L_T) - (D_{ai} - 2 \times 0.025) \right\} L_s \quad (3-9)$$

The length of the flux path through the armature core per pair of poles is

$$L_c = \frac{\pi}{4} \left\{ D_a - 2 L_T + D_{ai} - 2 \times 0.025 \right\} \quad (3-10)$$

A point on the armature core saturation curve may be determined in the following manner. First, assume a flux  $\phi$ . Then the flux density is

$$\text{Armature core density} = \frac{\phi}{A_c} \quad (3-11)$$

For this density, the ampere-turns per inch are obtained from the magnetization curve of the core material; the total ampere-turns for the entire armature core path are equal to the ampere-turns per inch multiplied by  $L_c$ .

Other points on the curve are similarly determined by assuming different values for  $\phi$ .

### 3.6 Yoke Saturation Curve

Refer to Figure 1-3. The yoke is assumed to be a hollow cylinder with an outer diameter  $D_o$  and an inner diameter of  $(D_o - 2Y)$ . As indicated in Article 3.2, the pole ampere-turns are taken care of by increasing the length of the yoke path. Thus,

$$L_y = \frac{1}{2} (\pi(D_o - Y)) \quad (3-12)$$

The cross-sectional area of the yoke is

$$A_y = (0.95 L_g) Y \quad (3-13)$$

A point on the yoke saturation curve may be found in the following way. First assume a flux  $\phi$ . Then the flux density is

$$\text{Yoke density } B_y = \frac{\phi}{2 A_y} \quad (3-14)$$

For this density, the ampere-turns per inch are obtained from the magnetization curve and the total ampere-turns are equal to the ampere-turns per inch multiplied by  $L_y$ .

The pole leakage flux may be accounted for by flux mapping. Since the yoke saturation curve is for both the yoke and poles, it is thought that the pole leakage flux may be taken into consideration by modifying the yoke saturation curve. A rough approximation is to multiply the ordinates of the yoke saturation curve by 0.94 (that is, allowing 6% for the leakage flux). A justification for this rough approximation is that the total no-load saturation curves as determined in Figure 3-1 gave satisfactory checks on the calculated total no-load saturation curves of the developed 400-watt and 200-watt generators. The modified curve shall be designated as the 0.94 yoke saturation curve.

### 3.7 Total No-load Saturation Curve

The total no-load saturation curve in Figure 3-1 is obtained by adding the ampere-turns for the armature core, teeth, 0.94 yoke, and gap for each value of  $\phi$ .

### 3.8 No-load $E_g$ vs NI Curve

The no-load  $E_g$  vs NI curve for any specified speed can be obtained with the aid of the no-load saturation curve in Figure 3-1 and the generated voltage equation

$$E_g = \frac{\phi n Z 10^{-8}}{60} \quad (1-2)$$

where  $\phi$  is obtained from the no-load saturation curve for any particular value of NI. Thus, a curve of  $E_g$  vs NI for any specified speed can be determined by using the corresponding  $\phi$ 's in equation (1-2) for the chosen NI's.

## 4. SHUNT FIELD WINDING

### 4.1 Introduction

The choice between short-shunt and long-shunt connection, the wire size of the shunt field coils, the number of shunt field turns, and the shunt field resistance will be considered in this section.

### 4.2 Short Shunt versus Long Shunt

The shunt field of a d-c cumulative-compound generator may be connected either short shunt or long shunt as indicated in Figure 4-1.

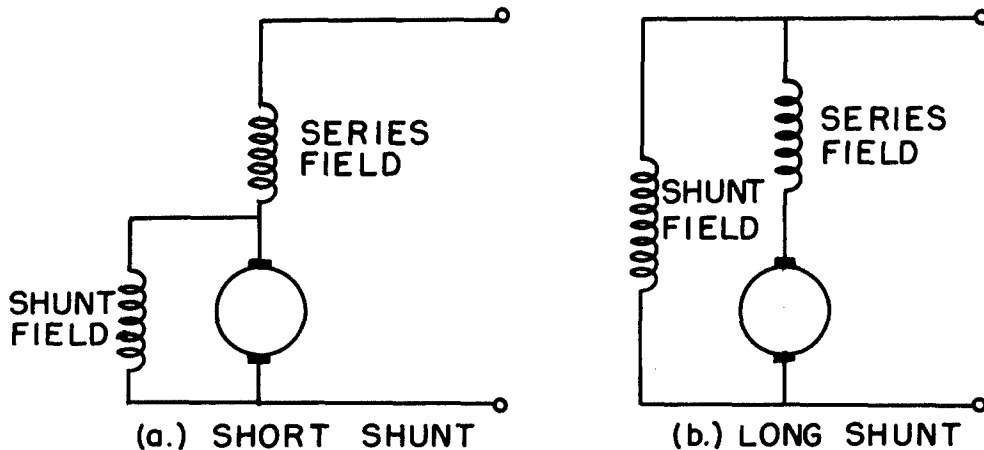


FIG. 4-1. SHUNT FIELD CONNECTIONS

Tests were run on three developed generators connected as both short and long shunt. Figure 4-2 shows typical terminal voltage versus load current curves for short-shunt and long-shunt connections. These curves indicated the following characteristics:

- (1) The no-load generated voltage for the long-shunt connection was slightly greater than that for the short-shunt connection. This could be attributed to the additional series field ampere-turns in the long-shunt connection.
- (2) The short-shunt connection gave a better flat compounding curve. This probably is due to the fact that the voltage across the shunt field of the short shunt case is not affected by the voltage drop of the series field.

On the basis of these terminal voltage versus load current curves, the developed generators were connected short shunt. Also, the design procedure will be limited to the short-shunt connection.

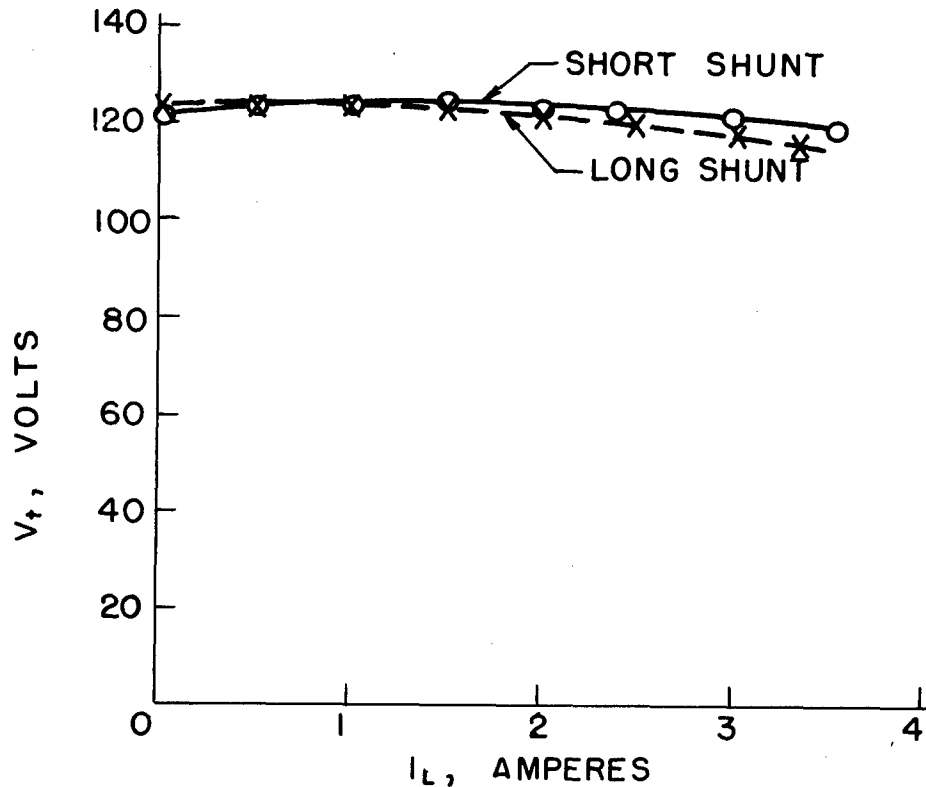


FIG. 4-2. TERMINAL VOLTAGE VS. LOAD CURRENT CURVES FOR A 400-WATT, 12250 RPM GENERATOR

#### 4.3 Wire Size of Shunt Field Coils

The wire size of shunt field coils may be estimated by first finding the resistance per inch of wire and then referring this resistance to wire tables for the wire size. This will now be considered.

The desired resistance of a mean shunt field turn may be obtained from the no-load  $E_g$  vs  $NI$  curve, discussed in Article 3.8 and given in Figure 4-3. It can be shown that the resistance of a mean shunt field turn is

$$R_{(LMT)_{sh}} = \frac{E_{g0}}{N_{sh} I_{sho}} \quad (4-1)$$

Since the generator is assumed to be flat-compounded, the no-load generated voltage  $E_{g0}$  may be considered as being equal to the rated terminal voltage  $(V_t)_{FL}$  plus two volts to allow for the brush and armature resistance drops. Then equation (4-1) may be written

$$R_{(LMT)_{sh}} = \frac{(V_t)_{FL} + 2}{N_{sh} I_{sho}} \quad (4-2)$$

Since  $R_{(LMT)sh}$  must satisfy the no-load condition, this resistance must be at the no-load temperature of the generator. For the developed generators, an average temperature rise of  $35^{\circ}\text{C}$  over ambient  $25^{\circ}\text{C}$  or a total of  $60^{\circ}\text{C}$  may be used as an approximate no-load temperature.

Knowing  $R_{(LMT)sh}$  at  $60^{\circ}\text{C}$ , the resistance per inch of wire can be found if the length of a mean turn can be estimated. Since the field coils are wound on a coil fixture, the dimensions of the fixture should be such so that the field coils can be inserted around the field poles.

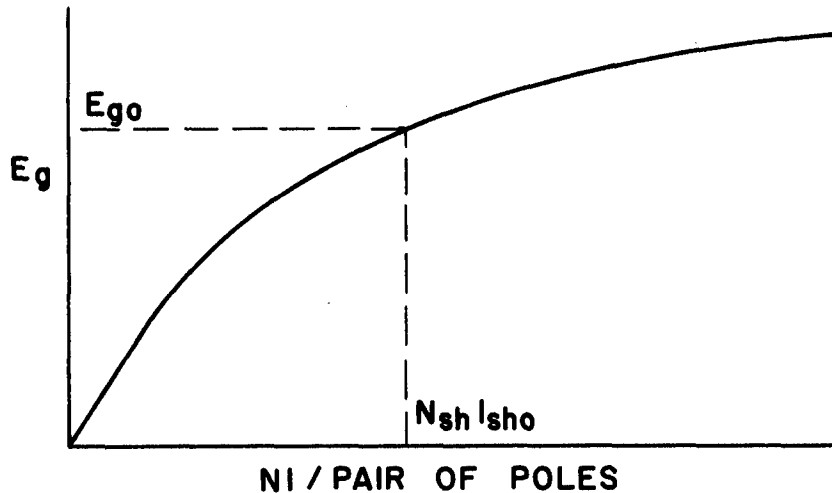


FIG. 4-3. NO-LOAD GENERATED VOLTAGE VERSUS AMPERE-TURNS PER PAIR OF POLES

As an approximation for the dimensions of the fixture, the length is usually  $3/16$  to  $1/4$  inch greater than the stack length  $L_s$  and the width is usually  $1/8$  to  $1/4$  inch greater than the width of the pole body. Thus, the first approximation of the length of a mean turn may be taken as the perimeter of the fixture. Then the resistance per inch at  $60^{\circ}\text{C}$  is

$$\rho_{60} = \frac{R_{(LMT)sh}}{\text{perimeter of fixture}} \quad (4-3)$$

This may be changed to the resistance per inch,  $\rho_t$ , at the temperature  $t$  used in the wire table, or

$$\rho_t = \frac{\rho_{60} (234.5 + t)}{(234.5 + 60)} \quad (4-4)$$

If  $\rho_t$  from equation (4-4) lies in between two wire sizes, the larger wire size should be used as it is possible to add external resistance to obtain the proper shunt field resistance.

#### 4.4 Number of Shunt Field Turns

Figure 4-3 shows that the ampere-turns  $N_{sh} I_{sho}$  are needed to produce the no-load generated voltage  $E_{go} = (V_t)_{FL} + 2$  for a particular generator. For short-shunt connection, the number of shunt field turns per pair of poles can be found if the no-load shunt field current can be determined, or

$$N_{sh} = \frac{N_{sh} I_{sho}}{I_{sho}} \quad (4-5)$$

The test results of each of the developed generators showed that the shunt field current remained practically constant from no load to full load. Since the cross-sectional area of the shunt field conductor for each of the developed generator is known, the current density can be calculated. This current density in the shunt field conductor may be used as an indication of the temperature rise of the generator. Figure 4-4 shows a curve between the current density  $J_{sh}$  in the shunt field conductors and the output power  $W_o$ . An approximate value for the shunt field current  $I_{sho}$  at no load may be obtained by multiplying the current density  $J_{sh}$  from Figure 4-4 by the cross-sectional area of the chosen wire size in Article 4.3.

With  $N_{sh} I_{sho}$  and  $I_{sho}$  known, the approximate number of shunt field turns can be calculated by equation (4-5).

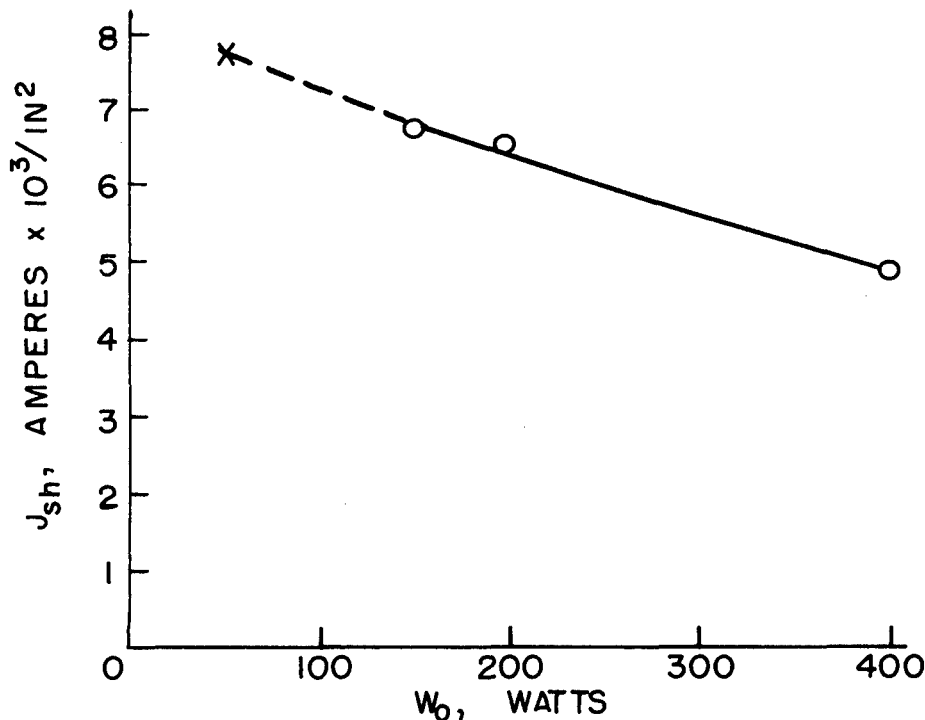


FIG 4-4. CURRENT DENSITY IN SHUNT FIELD CONDUCTORS VS. OUTPUT POWER

#### 4.5 Actual Shunt Field Resistance

The actual total shunt field resistance  $R_{sh}$  is equal to the product of the total length of wire of the entire shunt field winding and the resistance per inch at the no-load temperature (approximately  $60^{\circ} C$ ).

The wire size as determined in Article 4.3 will be satisfactory unless the perimeter in equation (4-3) differs greatly from the actual length of a mean turn.

A better estimate of the length of the mean turn may be obtained by knowing the cross-sectional area of the shunt field coil and the coil extension which will be defined below. With approximate values for the wire size and the number of turns, the cross-sectional area of a shunt field coil may be found by the relation

$$A_{sh} = \pi \left( \frac{D_{csh}}{2} \right)^2 \left( \frac{N_{sh}}{2} \right) \times \frac{1}{F_{sh}} \quad (4-6)$$

where

$D_{csh}$  = diameter of shunt field wire over the insulation.

$F_{sh}$  = fill factor of shunt field with an estimated value of about 0.75.

The coil extension is defined as the quotient obtained by dividing  $A_{sh}$  in equation (4-6) by the fixture thickness for the shunt field coil.

In determining the actual length of the mean turn, it is assumed that the mean turn is a turn midway between the inner and outer surfaces of the coil, and that this turn has a radius at the corners equal to one-half of the total coil extension, or

$$(LMT)_{sh} = \text{perimeter of fixture} + \pi \times \text{coil extension} \quad (4-7)$$

If this is too different from the perimeter of the fixture, then the work from equation (4-3) on must be repeated.

Thus, the actual total shunt field resistance  $R_{sh}$  is equal to the product of the final value of resistance per inch at approximately  $60^{\circ} C$  and the total length  $(LMT)_{sh} \times N_{sh}$ .

If  $R_{sh}$  is less than  $R(LMT)_{sh} \times N_{sh}$ , where  $R(LMT)_{sh}$  was found in equation (4-1), then external resistance must be added to the shunt field.

## 5. SERIES FIELD WINDING

### 5.1 Introduction

The series field coils will be designed primarily to satisfy the flat-compounding condition at full load. This involves the determination of the wire size, the number of turns, and the resistance of the series field. The final decision will depend on the shape of the calculated flat-compounding curve which will be considered in Section 6.

### 5.2 Series Field Wire Size.

Some of the factors which affect the choice of the series field wire size are the current density, the series field voltage drop as it influences the terminal voltage, and the available space to accommodate the series field coils. These factors particularly will affect the final choice of the series field wire size; that is, the wire size may be changed several times from the first estimate before the final choice is made. Thus, only an approximate first choice of the wire size will be sufficient.

Figure 5-1 shows a curve of current density in the series field ( $J_{se}$ ) versus output power ( $W_o$ ), which may be used as a guide in selecting the first approximate wire size. The data for this curve were obtained from the developed generators under full-load current conditions. The temperature rise at full load was about 55° C above an approximate ambient temperature of 25° C. For short-shunt connection, the full-load current is  $(I_L)_{FL}$  and the approximate cross-sectional copper area of the series field conductor is

$$A_{cse} = \frac{(I_L)_{FL}}{J_{se}} \quad (5-1)$$

The standard wire size should have a cross-sectional copper area which is closest to  $A_{cse}$ .

A first estimate of the wire size may also be made by selecting the smallest wire which has the current capacity to carry the rated current. This method involves the availability of a reliable wire table with current capacity of wires.

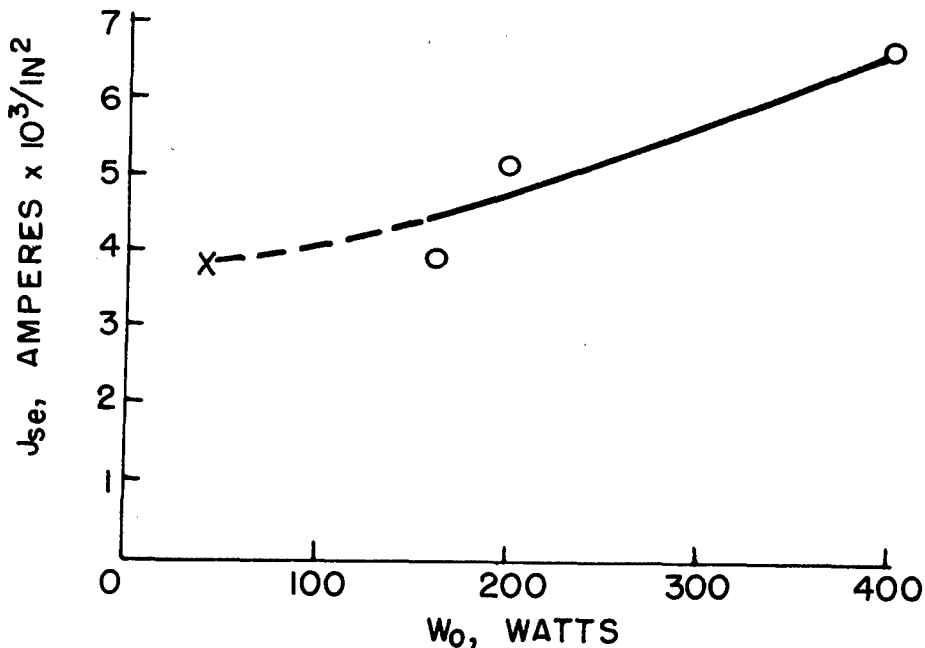


FIG. 5-1. CURRENT DENSITY IN SERIES FIELD CONDUCTORS VS. OUTPUT POWER

### 5.3 Armature Reaction Voltage Drop

When the brushes are located midway between the poles, the cross magnetizing ampere-turns resulting from the armature conductors lying directly under the pole faces tend to increase the flux at one pole tip and to decrease the flux at the other pole tip. Since at full load the generator operates on the saturated portion of the saturation curve, the cross magnetizing ampere-turns have a demagnetizing effect on the field. A method of calculating the decrease in generated voltage due to cross magnetization, which will be designated as armature reaction voltage drop  $V_{AR}$ , will now be presented.

For any specified load, the approximate value of cross magnetizing ampere-turns per pair of poles for a two-pole generator is

$$(NI)_c = \gamma \left(\frac{Z}{2}\right) I_a \times \frac{1}{2} \quad (5-2)$$

Typical individual saturation curves and a typical total no-load saturation curve were given in Figure 3-1. Article 3.8 showed how the total no-load saturation curve can be changed from a  $\phi - (NI)$  curve to a  $E_g - (NI)$  curve. Any combination of the individual saturation curves can also be changed from a  $\phi - (NI)$  curve to a  $E_g - (NI)$  curve. As an approximation, assume that the cross magnetizing ampere-turns are

effective only along the armature teeth and the air gap. Then the total no-load saturation curve and the teeth plus air gap curve in Figure 5-2 are used to determine the armature reaction voltage, or

$$V_{AR} = E_g \left( 1 - \frac{\text{area (A B' C' D)}}{\text{area (A B C D)}} \right) \quad (5-3)$$

Equation (5-3) assumes that the generated voltage  $E_g$  at any specified load is known. A method for estimating a value for  $E_g$  is given in the next article.

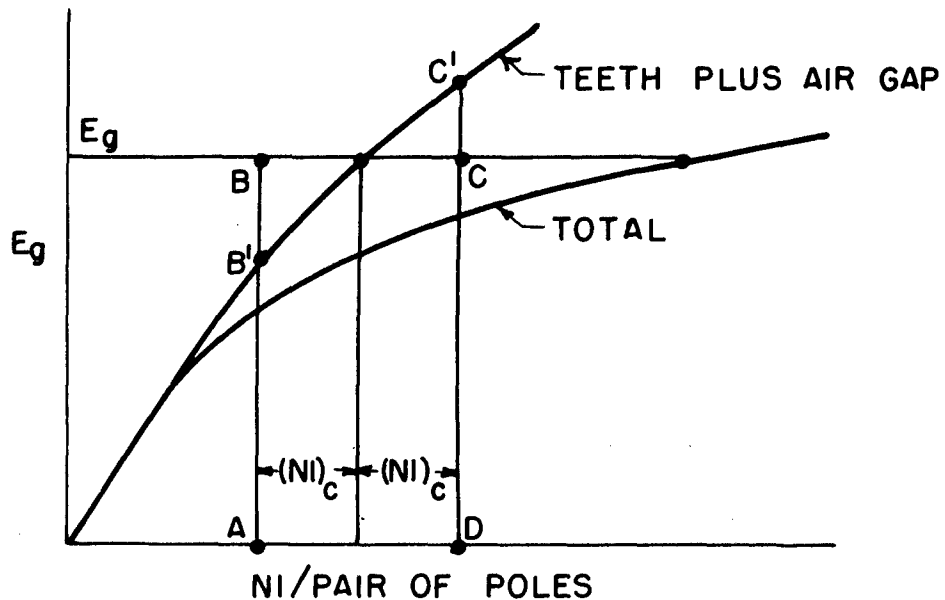


FIG. 5-2. NO-LOAD TOTAL AND TEETH PLUS AIR GAP GENERATED VOLTAGES VS. AMPERE-TURNS PER PAIR OF POLES

#### 5.4 Full-load Generated Voltage

The full-load generated voltage plays an important role in the design of the series field winding. It may be expressed by the relation:

$$E_g = V_t + I_L R_{se} + I_a R_a + V_{AR} + V_B \quad (5-3)$$

where the symbols should be interpreted to represent values at full-load condition.

The terminal voltage  $V_t$  and the line current  $I_L$  are the rated values of the generator. Since the shunt field current  $I_{sh}$  is practically constant from no load to full load as determined in Article 4.4, the full-load armature current is  $I_a = I_L + I_{sh}$ . The armature resistance  $R_a$  is given by equation (2-11). The series field resistance  $R_{se}$  will be discussed in the next article. The brush contact voltage drop  $V_B$  is assumed to have a relatively constant value of 2 volts. Since  $V_{AR}$  is dependent upon  $E_g$ , the value of  $E_g$  will be found by successive approximation; that is, when equation (5-3) is satisfied to a sufficient degree.

### 5.5 Number of Series Field Turns

The purpose of the series field is to add ampere-turns to the shunt field ampere-turns so that the terminal voltage  $V_t$  will not vary too much from no load to full load. That is, the generated voltage must be increased by the series field ampere-turns to compensate for the voltage drops in equation (5-3). The number of series field turns will be estimated at full-load condition since the generators are to be flat-compounded. The final choice of the series field turns may be affected by the variation of the terminal voltage  $V_t$  between no load and full load.

The number of series field turns will be determined by a cut-and-try process to satisfy equation (5-3). It may be considered that a final choice is obtained when equation (5-3) is satisfied to a sufficient degree. Throughout this cut-and-try process, the full-load armature drop  $I_a R_a$  and the brush drop  $V_B = 2$  are known and they are assumed to remain constant. Since  $V_{AR}$  and  $R_{se}$  will depend on the value of the generated voltage  $E_g$ , it is necessary to assume a value for  $E_g$  or to make an assumption whereby a starting value of  $E_g$  can be obtained. As a first approximation, assume  $I_L R_{se} = I_a R_a = V_{AR}$  so that equation (5-3) may be written

$$E_g' = V_t + 3I_a R_a + 2 \quad (5-4)$$

where  $V_t$  is the rated terminal voltage and the single prime indicates the first approximation. For  $E_g'$ , the armature reaction voltage  $V_{AR}$  is calculated as outlined in Article 5.3. The first estimate of the number of series field turns, with the aid of Figure 5-3, is

$$N_{se}' = \frac{N_{se}' I_L}{I_L} \quad (5-5)$$

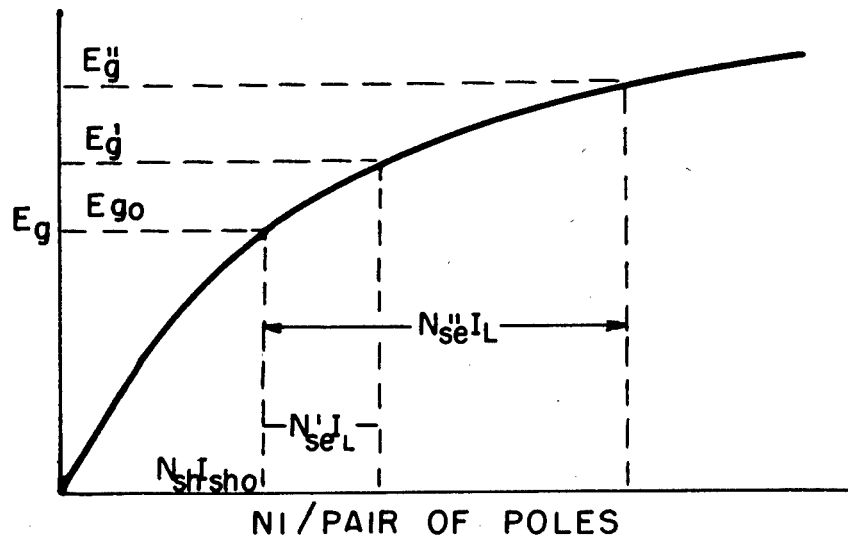


FIG. 5-3. NO-LOAD GENERATED VOLTAGE VS. AMPERE-TURNS PER PAIR OF POLES

Then the first approximation of the total series field resistance is

$$R_{se}' = N_{se}' (LMT)_{se} \rho_{se} \quad (5-6)$$

Substitution of known values in equation (5-3) gives for the first approximation

$$E_g' = V_t + I_L R_{se}' + I_a R_a + V_{AR}' + 2 \quad (5-7)$$

where  $V_t$  is the only unknown in this equation for full-load condition. If  $V_t$  is not sufficiently close to the rated terminal voltage of the generator, then a second approximation will be necessary.

The second approximation for the full-load generated voltage  $E_g''$  is

$$E_g'' = V_t + I_L R_{se}' + I_a R_a + V_{AR}' + 2 \quad (5-8)$$

where  $V_t$  is the rated terminal voltage and  $E_g''$  is the only unknown. Now with  $E_g''$  known,  $V_{AR}''$  can be calculated; also, with the aid of Figure 5-3,

$$N_{se}'' = \frac{N_{se}' I_L}{I_L} \quad (5-9)$$

and

$$R_{se}'' = N_{se}'' (LMT)_{se} \rho_{se} \quad (5-10)$$

Thus,

$$E_g'' = V_t + I_L R_{se}'' + I_a R_a + V_{AR}'' + 2 \quad (5-11)$$

where  $V_t$  is the only unknown in this equation for full-load condition. If  $V_t$  is still not sufficiently close to the rated terminal voltage, a third approximation will be necessary.

Sometimes, the following condition may arise. For a given wire size for the series field, it is possible that beyond a certain number of turns an increase of series field turns will cause a drop instead of an increase in the terminal voltage  $V_t$ ; that is, increasing the series field turns will not increase the terminal voltage to the desired value. This is due to the increase in series field voltage drop being greater than the additional generated voltage due to the additional series field ampere-turns. In such a case, the desired full-load terminal voltage  $V_t$  may be obtained by using a larger wire size and fewer series field turns to decrease the series field voltage drop.

## 6. TERMINAL VOLTAGE VS LOAD CURRENT CURVE

### 6.1 Introduction

The object of this section is to describe a procedure for calculating points on the terminal voltage vs load current curve. Such a curve will show the variation of terminal voltage from no load to full load.

### 6.2 Terminal Voltage vs Load Current Curve

A procedure to calculate the terminal voltage  $V_t$  at any load current  $I_L$  will now be considered. The terminal voltage can be obtained from the expression.

$$V_t = E_g - (I_L + I_{sh}) R_a - I_L R_{se} - V_{AR} - 2 \quad (6-1)$$

which is similar to equation (5-3) except that here the symbols represent values at a particular load current. The problem becomes one of choosing different values for  $I_L$  and solving for the corresponding  $V_t$ 's.

It is assumed that  $N_{sh}$  and  $N_{se}$  are known and that the shunt field current  $I_{sh}$  is practically constant from no load to full load, as determined in Article 4.4. The resistances  $R_a$  and  $R_{se}$  at the different load currents can be found with the assumption that the generator temperature varies linearly from a no-load temperature of 60° C to a full-load temperature of 80° C. The generated voltage  $E_g$  is found from the total no-load generated voltage curve in Figure 6-1 for the ampere-turns  $(N_{sh}I_{sh}) + (N_{se}I_L)$ . The armature reaction voltage drop  $V_{AR}$  is found as outlined in Article 5.3.

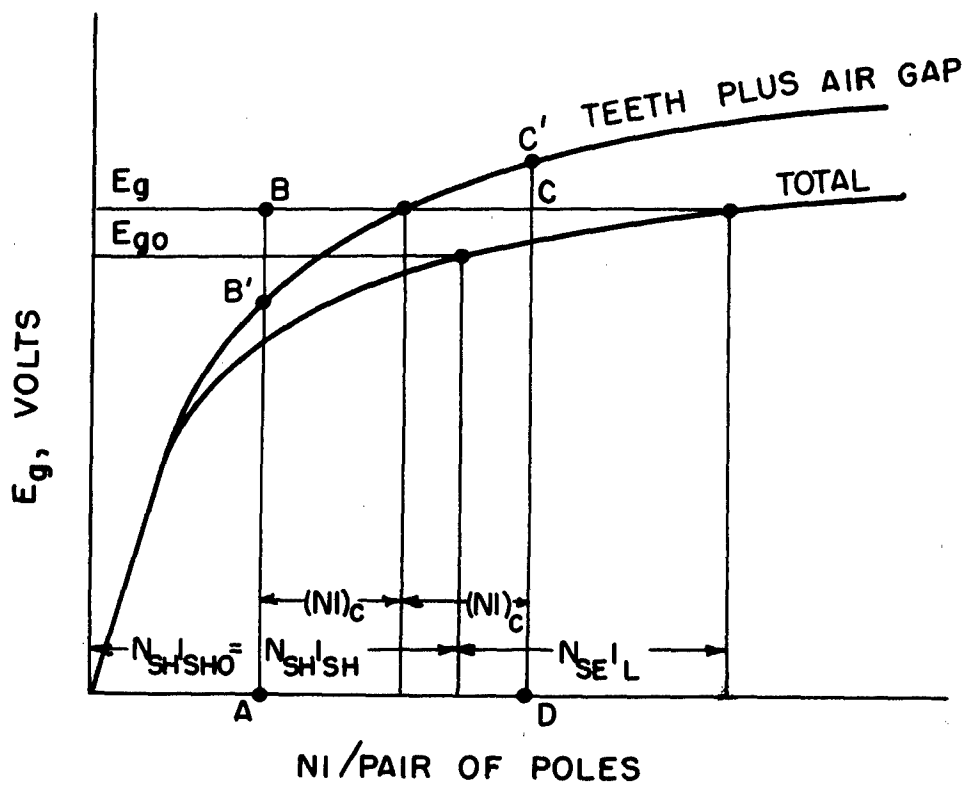


FIG. 6-1. GENERATED VOLTAGE VS. AMPERE TURNS PER PAIR OF POLES

## BIBLIOGRAPHY

1. Gray, Alexander, Electrical Machine Design, McGraw-Hill Book Company, Inc., New York, 1926.
2. Kuhlmann, John H., Design of Electrical Apparatus, John Wiley & Sons, Inc., New York, 1940.
3. Siskind, Charles S., Direct-Current Armature Windings, McGraw-Hill Book Company, Inc., New York, 1949.
4. Spreadbury, F. G., Aircraft Electrical Engineering, Sir Isaac Pitman & Sons, Ltd., London, 1947.
5. Spreadbury, F. G., Fractional H. P. Electric Motors, Sir Isaac Pitman & Sons, Ltd., London, 1951.